

Article

Discovery of carbohybrid-based 2-aminopyrimidine analogues as a new class of rapid-acting antimalarial agents using image-based cytological profiling assay

Sukjun Lee, Donghyun Lim, Eunyoung Lee, Nakyung Lee, Hong-gun Lee, Jonathan Cechetto, Michel Liuzzi, Lucio H. Freitas-Junior, Jin Sook Song, Myung Ae Bae, Sangmi Oh, Lawrence Ayong, and Seung Bum Park

J. Med. Chem., **Just Accepted Manuscript** • DOI: 10.1021/jm5009693 • Publication Date (Web): 19 Aug 2014

Downloaded from <http://pubs.acs.org> on August 23, 2014

Just Accepted

“Just Accepted” manuscripts have been peer-reviewed and accepted for publication. They are posted online prior to technical editing, formatting for publication and author proofing. The American Chemical Society provides “Just Accepted” as a free service to the research community to expedite the dissemination of scientific material as soon as possible after acceptance. “Just Accepted” manuscripts appear in full in PDF format accompanied by an HTML abstract. “Just Accepted” manuscripts have been fully peer reviewed, but should not be considered the official version of record. They are accessible to all readers and citable by the Digital Object Identifier (DOI®). “Just Accepted” is an optional service offered to authors. Therefore, the “Just Accepted” Web site may not include all articles that will be published in the journal. After a manuscript is technically edited and formatted, it will be removed from the “Just Accepted” Web site and published as an ASAP article. Note that technical editing may introduce minor changes to the manuscript text and/or graphics which could affect content, and all legal disclaimers and ethical guidelines that apply to the journal pertain. ACS cannot be held responsible for errors or consequences arising from the use of information contained in these “Just Accepted” manuscripts.



1
2
3
4
5
6
7
8
9
10
11
12
13
14
15
16
17
18
19
20
21
22
23
24
25
26
27
28
29
30
31
32
33
34
35
36
37
38
39
40
41
42
43
44
45
46
47
48
49
50
51
52
53
54
55
56
57
58
59
60

Discovery of carbohybrid-based 2-aminopyrimidine analogues as a new class of rapid-acting antimalarial agents using image-based cytological profiling assay

Sukjun Lee,^{a,†} Donghyun Lim,^{b,†} Eunyoung Lee,^a Nakyung Lee,^c Hong-gun Lee,^d Jonathan Cechetto,^d Michel Liuzzi,^a Lucio H. Freitas-Junior,^c Jin Sook Song,^e Myung Ae Bae,^e Sangmi Oh,^f Lawrence Ayong,^{a} and Seung Bum Park^{b,g*}*

^aEarly Discovery Program, Institut Pasteur Korea, Seongnam-si, Gyeonggi-do 463-400, Korea

^bWCU Department of Biophysics and Chemical Biology, Seoul National University, Seoul 151-747, Korea

^cCenter for Neglected Diseases Drug Discovery (CND3), Institut Pasteur Korea, Gyeonggi-do 463-400, Korea

^dCenter for Core Technologies, Institut Pasteur Korea, Institut Pasteur Korea, Gyeonggi-do 463-400, Korea

^eDrug Discovery Platform Technology Group, Drug Discovery Division, Korea Research Institute of Chemical Technology, Daejeon 305-600, Korea

^fMedicinal Chemistry and Chemical Biology Group, Institut Pasteur Korea, Gyeonggi-do 463-400, Korea

^gDepartment of Chemistry, Seoul National University, Seoul 151-747, Korea

ABSTRACT

New antimalarial agents that exhibit multi-stage activities against drug-resistant strains of malaria parasites represent good starting points for developing next generation antimalarial therapies. To facilitate the progression of such agents into the development phase, we developed an image-based parasitological screening method for defining drug effects on different asexual life cycle stages of *P. falciparum*. High-throughput screening of a newly assembled diversity-oriented synthetic library using this approach led to the identification of carbohybrid-based 2-aminopyrimidine compounds with fast-acting growth inhibitory activities against three laboratory strains of multi-drug resistant *P. falciparum*. Our structure-activity relationship study led to the identification of two derivatives (**8aA** and **11aA**) as the most promising antimalarial candidates (mean EC₅₀ of 0.130 and 0.096 μM against all three *P. falciparum* strains, selectivity indices >600, microsomal stabilities >80%, and mouse malaria ED₅₀ values of 0.32 and 0.12 mg/kg/day, respectively) targeting all major blood stages of multi-drug-resistant *P. falciparum* parasites.

INTRODUCTION

With nearly a million deaths annually and over 219 million hospital cases each year, malaria remains a serious public health problem, particularly in the high transmission areas of Sub-Saharan Africa, Southeast Asia, and Latin America.¹⁻³ The disease is caused by mosquito-borne protozoan parasites of the genus *Plasmodium*; five species of which are known to infect humans (*P. falciparum*, *P. vivax*, *P. ovale*, *P. malariae*, and *P. knowlesi*).^{4,5} In the absence of vaccines with operational utilities against the disease, accurate diagnosis and treatment with available antimalarial regimens alongside effective vector control measures remain the best hope of controlling the disease globally.⁶⁻⁸

Plasmodium parasites, however, exhibit a high propensity to rapidly developed resistance against newly introduced medicines, necessitating as such a continuous search and development of new antimalarial agents to combat emerging resistant strains.^{9,10} To stop the spread of multi-drug resistance worldwide, the World Health Organization recommends the use of artemisinin-based combination treatments for all uncomplicated malaria cases globally. A key inclusion benefit of artemisinin in the current combinations lies in its rapid-acting multi-stage activities against most drug-resistant strains of *Plasmodium* parasites.¹¹ Unfortunately, parasite resistance to artemisinin has been inevitable as revealed by the recent emergence and spread of drug-tolerant parasites along the Thai-Cambodian borders in South East Asia.^{12,13}

This dire situation calls for the immediate development, preferably, of non-artemisinin-based compounds with fast-acting, long-lasting and multi-stage activities capable of reducing treatment durations while also improving patient compliances.¹¹ Indeed, compared to slow-acting single-target drugs such as pyrimethamine (antifolate), sulfadoxine (antifolate), and atovaquone (cytochrome bc1 complex inhibitor), anti-malarial compounds that exhibit fast-acting and

1
2
3 pleiotropic activities similar to that of artemisinin and chloroquine are expected to display shorter
4
5 parasite clearance times (PCTs), increased useful therapeutic lives (UTLs), and high parasitaemia
6
7 reduction ratios (PRR) with net effects being increased cure rates and mitigation of resistance
8
9 development.^{10,14,15}
10
11

12
13 Discovering new therapeutic agents in malaria requires a combination of new chemical libraries
14
15 and innovative screening technologies. Indeed, plausible efforts by both pharmaceutical industries
16
17 and academic research institutions recently had led to the identification of several structurally
18
19 diverse antimalarial compounds, some of which are under scrutiny by partnerships such as the
20
21 Medicine for Malaria Ventures (MMV) for inclusion into the lead discovery chain.
22
23

24
25 Recently, we described the development of an automated image-based screening system for the
26
27 quantitative detection and classification of *P. falciparum* life cycle stages in a 384-culture well
28
29 format.¹⁶ In parallel, we constructed a small molecule library of over 4,000 drug-like compounds
30
31 containing 60 distinct core structures using a privileged-substructure-based diversity-oriented
32
33 synthetic (pDOS) approach.¹⁷ By using the above image-based system first as a growth inhibition
34
35 screening assay and then as a cytological profiling tool, we identified carbohybrid-based 2-
36
37 aminopyrimidines from our pDOS library as a new class of anti-malarial compounds with potent
38
39 activities against three laboratory strains of multiple drug-resistant *P. falciparum*. In fact, we
40
41 recently reported the synthesis of stereochemically enriched acyclic polyols fused with various
42
43 privileged heterocycles from naturally abundant carbohydrates and named them as
44
45 “carbohybrids”.¹⁸ On the basis of structure-activity relationship studies, we identified 2-
46
47 aminopyrimidine analogues (**8aA** and **11aA**) of the initial hit compounds as the most promising
48
49 candidates given their high *in vitro* potency, and excellent *in vivo* PK properties and efficacy in a
50
51 mouse malaria model.
52
53
54
55
56
57
58
59
60

RESULTS AND DISCUSSION

A Novel Image-based Cytological Profiling Assay. *Plasmodium* parasites exhibit a complex life cycle that involves multiple parasite stages and forms, which display variable degrees of sensitivity to most antimalarial compounds.^{14,19,20} To facilitate the discovery and development of new therapies that target existing strains of drug-resistant *P. falciparum*, we developed a cytological profiling method using our previously reported image-based screening system.¹⁶ This assay relies on the quantitative detection of each major blood form (early rings, late rings, trophozoites, and schizonts) of *P. falciparum* parasites in a 384-well format based on the numbers and sizes of detectable nuclear condensation spots in infected erythrocytes. In this assay, all host cells are stained with wheat germ agglutinin-AlexaFluor 488 conjugate whereas individual parasites in infected erythrocytes are identified using the nuclear stain DAPI. The assay also employs the fluorescent dye Mitotracker red CMXRos to stain and discriminate functional mitochondria in live parasites and disrupted mitochondria in dead parasites. A major advantage of our image-based system is in its ability to quantify drug activities on the basis of total culture parasitaemia, and to determine each parasite stage proportion in an automated fashion. The cytological profiling approach as developed in this study involves parasite treatment at well-defined time-points in the parasite's intraerythrocytic life cycle, and comparison of the resulting stage accumulation indices following 36 or 24 h of drug pressure. We confirmed the reliability of this approach by profiling the stage specificities of four mechanistically known antimalarial agents using three different drug resistant lines of *P. falciparum* (Figure 1). Consistent with their known modes of actions,^{14,19,21–27} our data show that artemisinin (ART) and chloroquine (CQ) are fast-acting in inhibiting early and late ring development to the mid-trophozoite stage, but that these

1
2
3 compounds are only weakly active against trophozoite development to the schizont stages (Figure
4
5
6 1A). Indeed, at clinically relevant concentrations (peak plasma concentrations of ~2 μM for ART
7
8 and 1–10 μM for CQ),^{28–30} both chloroquine and artemisinin are known to rapidly inhibit cell cycle
9
10 development in malaria parasites resulting in parasite clearance times of <24 h for both drugs.
11

12
13 *Trans*-Epoxy succinyl-L-leucylamido-(4-guanidino)butane (E64) on its part inhibited early ring
14
15 development and schizont maturation, whereas *N*-acetylglucosamine (GlcNAc) was only weakly
16
17 effective at inhibiting early ring development in all three parasite lines (Figure 1A). As shown in
18
19 Figure 1B, ART, E64 and GlcNAc also produced significant decreases in culture parasitaemia
20
21 when added at the 42 h time-point for 24 h. Indeed, both ART and E64 gave significantly high
22
23 schizont accumulation indices, indicating rapid inhibition of schizont maturation and/or merozoite
24
25 egress, whereas GlcNAc reduced culture parasitaemia without a significant retention of schizonts.
26
27 This later indicates that GlcNAc predominantly acts on extracellular merozoites, inhibiting host
28
29 cell entry as reported previously.²¹ Taken together, the above results demonstrated the ability of
30
31 our cytological profiling approach to quantify the stage-specificities of antimalarial agents at
32
33 different time-points during the parasite's asexual developmental cycle with high reliability and in
34
35 a high-throughput screening format.
36
37
38
39

40
41 **Discovery of Carbohybrid-based Aminopyrimidines as a New Antimalarial Drug Class.** To
42
43 identify antimalarial compounds with novel modes of action, we screened an in-house 3,980-
44
45 member small molecule library using our image-based parasitological assay system and the
46
47 chloroquine/pyrimethamine-resistant *P. falciparum* K1 strain. This initial screen resulted in 89 hit
48
49 compounds (hit rate of 2.4%) that inhibited parasite growth by >90% when used at 5 μM final
50
51 concentrations and exhibited EC_{50} values less than 2 μM . Counter-screening of these initial hits
52
53 against two other drug-resistant parasite strains (W2 and HB3) identified the carbohybrid
54
55
56
57
58
59
60

1
2
3 frameworks containing 2-aminopyrimidine moiety **1** (SNU3701) and **2** (SNU3662)³¹ that
4 displayed similar EC₅₀ values (less than 1 μM) against all three *P. falciparum* strains (Table 1).
5
6

7
8 Dose-responsive cytotoxicity analyses of the above compounds using three different human cell
9 lines (HepG2, THP-1, and U2OS) gave high selectivity indices in all three cell lines (Table 1),
10 indicating *in vitro* safety towards these cell lines. Cytological profiling of the compounds using
11 drug-resistant *P. falciparum* K1 parasites revealed that carbohybrid-based 2-aminopyrimidine
12 analogues (**1** and **2**) exhibit fast-acting antimalarial activities by inhibiting further development of
13 early rings, late rings, and mid-trophozoite stage parasites when treated at the 6, 18, or 30 h post-
14 invasion (Figure 2A and 2B). These two compounds, however, did not significantly affect parasite
15 mitochondrial integrity as assessed by using the mitochondrial membrane potential indicator,
16 Mitotracker Red CMXRos (Figure S1, Supporting Information).
17
18
19
20
21
22
23
24
25
26
27
28

29 Treatment of the parasites at the 42-hpi time-point resulted in a parasitaemia reduction index of
30 0.52 for **1** and 0.46 for **2**, and schizont accumulation index of approximately 2.4 for each compound.
31
32 These results indicate that both compounds are fast acting in inhibiting schizont maturation and/or
33 merozoite egress from the infected erythrocytes leading to accumulation of schizonts in culture.
34
35 Collectively, we concluded that carbohybrid-based 2-aminopyrimidine analogues are a novel class
36 of fast acting blood-stage antimalarial compounds on the basis of their ability to block cell cycle
37 progression from the treated parasite stages.
38
39
40
41
42
43
44
45

46 Encouraged by these findings, we constructed a focused library of 2-aminopyrimidine-based
47 carbohybrids using our divergent synthetic strategy.¹⁸ As shown in Scheme 1, 6-hydroxyl groups
48 in D-galactal (**3a**, R¹ = OPMB, R² = H) and D-glucal (**3b**, R¹ = H, R² = OPMB) were selectively
49 protected with trityl group to afford **4a** and **4b**. *p*-Methoxybenzyl (PMB) protection of secondary
50 hydroxyl groups, followed by Vilsmeier-Haack formylation, resulted in the 2-*C*-formyl glycals,
51
52
53
54
55
56
57
58
59
60

1
2
3 **6a** and **6b**. The condensation of these intermediates (**6a** and **6b**) with dinucleophiles and the
4
5 subsequent ring opening yielded the carbohybrid scaffolds **7** consisting of diverse heterocyclic
6
7 moieties (pyrimidine, pyrazolopyrimidine, and pyrazole). Sequential modifications of functional
8
9 groups through mesylation, trityl deprotection, and azide substitution allowed the formation of
10
11 carbohybrids **8**, **9** and **10**, respectively, with different appendices. Finally, the primary hydroxyl
12
13 group in **10** was transformed via tritylation, benzylation, and mesylation to afford analogues **11**,
14
15 **12** and **13**, respectively. The modification of **7bA** with PMB group, instead of trityl group at the
16
17 R⁵ position, and the subsequent *O*-mesylation yield analogues **14bA** and **15bA**, respectively
18
19 (Scheme S1, Supporting Information).
20
21
22
23

24
25 Given the occurrence of 2-aminopyrimidine heterocycles in our carbohybrid-based hit
26
27 compounds, we investigated the antimalarial activities of carbohybrids that contained pyrimidine
28
29 (**2**, **7aA**, **7aC**), pyrazolopyrimidine (**7aD**), and pyrazole (**7aE**) in their substructures. As shown in
30
31 Table 2, carbohybrid analogues containing all three heterocycles exhibited antimalarial activities
32
33 (EC₅₀ < 1 μM) against chloroquine/pyrimethamine-resistant *P. falciparum* strain K1.
34
35 Stereochemical modifications at the R¹ and R² positions, which was achieved by using different
36
37 glycals (**3a** or **3b**) as starting material, minimally affected their inhibitory activities. However, the
38
39 galactal-derived compounds (**7aA**, **7aE**, **8aA**, **8aE**, and **11aA**) exhibited slightly higher
40
41 antimalarial activities compared with those of the glucal-based derivatives (**7bA**, **7bE**, **8bA**, **8bE**,
42
43 and **11bA**). The modification at the primary hydroxyl group (R⁵) appeared critical for the
44
45 antimalarial activity. For example, the introduction of bulky hydrophobic moieties such as the
46
47 trityl group in **8aA** and **11aA** allowed a more than 50-fold enhancement in antimalarial activities
48
49 compared with those of unmodified hydroxyl version in carbohybrid analogues **9aA** and **10aA**.
50
51 Consistent with this observation, the introduction of benzyl group (**12aA**) enhanced their
52
53
54
55
56
57
58
59
60

1
2
3 antimalarial activities, albeit not as much as those in trityl-containing carbohybrid derivatives.
4
5 Importantly, *O*-mesylation as exemplified in derivative **8aA** and azide substitution at the R⁴
6
7 position of the carbohybrid chain (e.g. **11aA**) enhanced the class antimalarial activities. On the
8
9 basis of their potent *in vitro* activities (EC₅₀: 104–147 nM and 80–96 nM, respectively, against all
10
11 three drug-resistant parasite strains), fast-acting activities against ring, trophozoite and schizont
12
13 development (Figure S2, Supporting Information), and high selectivity indices (S.I. >680 for **8aA**
14
15 and >1000 for **11aA**), the above two carbohybrid-based 2-aminopyrimidine derivatives were
16
17 selected for further pharmacokinetics analyses.
18
19
20
21

22 Our candidate compounds **8aA** and **11aA** were examined for their microsomal stability (n = 3).
23
24 As shown in Table 3, both compounds showed excellent *in vitro* metabolic stability, with greater
25
26 than 80% compound remaining after 30 min in human and mouse liver microsomes. In addition,
27
28 carbohybrid-based 2-aminopyrimidine derivative **8aA** at the dose of 1 and 5 mg/kg showed
29
30 excellent pharmacokinetic behavior after intraperitoneal (i.p.) injection in SD male rats (n = 5),
31
32 with rapid absorption (time to peak concentration [T_{max}] of 1 h and maximum concentration [C_{max}]
33
34 of 1.80±0.40 and 12.9±9.30 g/mL, respectively) and stable plasma concentration of more than 0.10
35
36 and 0.15 µg/mL over 24 h (Figure S3, Supporting Information). The area under the curve (AUC)
37
38 of **8aA** and **11aA** confirmed the excellent pharmacokinetic property, which assures their
39
40 pharmacological activities *in vivo*.
41
42
43
44
45

46 **Novel *In Vivo* Antimalarial Activity of 8aA and 11aA in a Mouse Malaria Model.** To assess
47
48 the *in vivo* efficacy of carbohybrid-based antimalarial candidates (**8aA** and **11aA**), groups of *P.*
49
50 *chabaudi*-infected mice were treated by i.p. injection on Day 1 (trophozoite-stage parasites) to Day
51
52 3 post-infection using fixed doses of 0.03, 0.3, 3, 10 or 30 mg/kg for each compound. Percent
53
54 inhibitions of parasite growth in treated groups relative to the control parasitaemia on Day 4 were
55
56
57
58
59
60

1
2
3 then used in probit analyses of compounds' effects. As shown in Figure 3, both candidate
4
5 compounds (**8aA** and **11aA**) displayed significant *in vivo* antimalarial activities in a dose-
6
7 dependent manner. Based on the probit 5-response point, the compound's ED₅₀ against *P. chabaudi*
8
9 infection were estimated to be 0.32 mg/kg for **8aA** and 0.12 mg/kg for **11aA**. As observed by light
10
11 microscopy examination of thin smears, mice treatment with either **8aA** or **11aA** at doses greater
12
13 than 3 mg/kg resulted in a significant reduction in blood parasitaemia, and accumulation of ring-
14
15 stage parasites in the infected mice unlike trophozoite stage parasites in untreated controls (Figure
16
17 S4, Supporting Information). These findings are consistent with the 24 h life cycle of
18
19 synchronously developing *P. chabaudi* in mice, and indicate a fast acting (approximately 12 h
20
21 post-i.p. drug administration) *in vivo* antimalarial activity of the compounds. Collectively, the
22
23 above data demonstrate clearly the therapeutic potential of the carbohybrid-based 2-
24
25 aminopyrimidine **8aA** and **11aA** in a mouse malaria model.
26
27
28
29
30
31
32
33

34 CONCLUSIONS

35
36 Herein, we reported the development and application of a novel image-based cytological
37
38 profiling assay for the discovery of novel antimalarial agents. Using this screening system, we
39
40 identified carbohybrid-based 2-aminopyrimidines from 4,000-membered in-house pDOS small
41
42 molecule library as a new class of blood-stage antimalarial agents. Based on our *in vitro* biological
43
44 evaluation of their synthetic analogues, we optimized our initial hit compound to **8aA** and **11aA**
45
46 as antimalarial candidates with excellent potency, high selectivity indices, and rapid acting
47
48 activities against all major asexual parasite forms. Finally, these lead compounds exhibited
49
50 favorable pharmacokinetic properties and fast-acting *in vivo* efficacy. We conclude that these
51
52 carbohybrid-based 2-aminopyrimidine analogues **8aA** and **11aA** can be a promising class of
53
54
55
56
57
58
59
60

1
2
3 antimalarial agents with potentials for clinical use against uncomplicated and/or severe malaria
4 cases.
5
6

7
8
9
10 **EXPERIEMNTAL SECTION**
11

12 **Chemistry.** All commercially available reagents and solvents were used without further
13 purification unless noted otherwise. ^1H and ^{13}C NMR spectra were recorded on Varian Inova-500
14 [Varian Assoc.] or Agilent 400-MR DD2 [Agilent] instruments. Chemical shifts were reported in
15 ppm relative to tetramethylsilane (TMS) as an internal standard or residual solvent peak (CDCl_3 ;
16 ^1H : $\delta = 7.26$ ppm; ^{13}C : $\delta = 77.23$ ppm). Multiplicity was indicated as follows: s (singlet), d
17 (doublet), t (triplet), q (quartet), m (multiplet), dd (doublet of doublet), dt (doublet of triplet), td
18 (triplet of doublet), brs (broad singlet). Coupling constants are reported in hertz. HRMS analyses
19 were conducted at the National Center for Inter-University Research Facilities in Seoul National
20 University by fast atom bombardment (FAB) method. Routine mass spectrometric analysis was
21 performed on a Finnigan Surveyor MSQ Plus LC/MS [Thermo] by electrospray ionization (ESI)
22 method. Purity of the compounds was determined using the Finnigan Surveyor MSQ Plus LC/MS
23 [Thermo] equipped with a Hypersil Gold column and photodiode array detector, or a Shimadzu
24 SCL-10AVP HPLC [Shimadzu] equipped with a VP-ODS column and 254 nm detector. All the
25 final compounds were >95% pure. The conversion of starting materials was monitored by thin-
26 layer chromatography (TLC) using pre-coated glass-backed plates (silica gel 60; $F_{254} = 0.25$ mm),
27 and the reaction components were visualized by observation under UV light (254 and 365 nm) or
28 by treatment of TLC plates with visualizing agents such as KMnO_4 , phosphomolybdic acid and
29 ceric sulfate followed by heating. Products were purified by flash column chromatography on
30 silica gel (230–400 mesh) using a mixture of EtOAc/hexane or MeOH/ CH_2Cl_2 as eluents.
31
32
33
34
35
36
37
38
39
40
41
42
43
44
45
46
47
48
49
50
51
52
53
54
55
56
57
58
59
60

1
2
3 Synthetic methods and spectroscopic data for **2**, **6a**, **6b**, **7aA–7bA** and **10aA–10aD** were reported
4
5 by Lim et al.¹⁸
6
7

8 **Synthesis of a Glucal-derived Pyrazole-containing Carbohybrid (7bE).** A solution of **6b**
9 (100 mg) in tetrahydrofuran (3 mL) was added to a stirred solution of methylhydrazine sulfate (2
10 equiv.) and K₂CO₃ (5 equiv.) in ethanol (3 mL). The reaction mixture was stirred at room
11 temperature for 15 h. The solvent was removed under reduced pressure and the residue was
12 partitioned between ethyl acetate and water. The aqueous layer was extracted with ethyl acetate
13 twice, and the combined organic layer was dried over anhydrous Na₂SO₄(s). The filtrate was
14 condensed under reduced pressure and subjected to flash column chromatography. White solid.
15 Yield: 56%; ¹H NMR (400 MHz, CDCl₃) δ 7.43–7.40 (m, 7H), 7.29–7.21 (m, 10H), 7.13 (d, *J* =
16 8.6 Hz, 2H), 6.98 (d, *J* = 8.6 Hz, 2H), 6.80 (d, *J* = 8.6 Hz, 2H), 6.76 (d, *J* = 8.6 Hz, 2H), 4.52 (d, *J* =
17 3.9 Hz, 1H), 4.43 (d, *J* = 11.7 Hz, 1H), 4.31 (s, 2H), 4.11 (d, *J* = 11.7 Hz, 1H), 3.94–3.90 (m,
18 1H), 3.85 (s, 3H), 3.783 (s, 3H), 3.778 (s, 3H), 3.69 (dd, *J* = 6.5, 3.7 Hz, 1H), 3.26–3.23 (m, 1H),
19 3.19–3.15 (m, 2H); ¹³C NMR (100 MHz, CDCl₃) δ 159.4, 159.3, 144.1, 139.3, 130.3, 130.1, 129.9,
20 129.84, 129.80, 128.9, 128.0, 127.2, 118.9, 114.0, 113.7, 86.6, 80.5, 73.7, 73.2, 70.8, 70.2, 64.8,
21 55.43, 55.42, 39.2; HRMS (FAB+) *m/z* calculated for C₄₃H₄₄N₂O₆ [M+H]⁺: 685.3278; found:
22 685.3282.
23
24
25
26
27
28
29
30
31
32
33
34
35
36
37
38
39
40
41
42

43 **General Synthetic Procedure for *O*-Mesylated Carbohybrids (8).** Triethylamine (3 equiv.)
44 and methanesulfonyl chloride (2 equiv.) were added to a stirred solution of **7** (100 mg) in
45 anhydrous CH₂Cl₂ at 0 °C. The mixture was stirred at 0 °C for 2 h, diluted with CH₂Cl₂ and washed
46 with brine. The aqueous layer was extracted with CH₂Cl₂, and the combined organic layer was
47 dried over anhydrous Na₂SO₄(s). The filtrate was condensed under reduced pressure and subjected
48 to flash column chromatography. **8aA:** Prepared from **7aA** as a white solid. Yield: 99%; ¹H NMR
49
50
51
52
53
54
55
56
57
58
59
60

(400 MHz, CDCl₃) δ 8.18 (s, 2H), 7.39–7.37 (m, 6H), 7.31–7.22 (m, 11H), 6.90 (d, *J* = 8.6 Hz, 2H), 6.80 (d, *J* = 8.6 Hz, 2H), 6.71 (d, *J* = 8.6 Hz, 2H), 4.99 (dt, *J* = 6.7, 3.5, 1H), 4.32–4.22 (m, 4H), 4.10 (d, *J* = 10.6 Hz, 1H), 3.91 (dd, *J* = 6.7, 4.3 Hz, 1H), 3.76 (s, 3H), 3.75 (s, 3H), 3.35 (dd, *J* = 10.8, 3.3 Hz, 1H), 3.20 (s, 6H), 3.18–3.16 (m, 1H), 2.92 (s, 3H); ¹³C NMR (100 MHz, CDCl₃) δ 162.4, 159.5, 158.2, 143.4, 130.4, 130.1, 129.8, 129.3, 128.7, 128.2, 127.5, 118.0, 114.0, 113.8, 87.4, 81.5, 80.4, 76.0, 75.3, 70.0, 63.5, 55.5, 55.4, 38.9, 37.4, 31.7; HRMS (FAB+) *m/z* calculated for C₄₆H₄₉N₃O₈S [M+H]⁺: 804.3319; found: 804.3315.

General Synthetic Procedure for Detritylated Carbohyrids (9). To a stirred solution of **8** (100 mg) in methanol, *p*-toluenesulfonic acid (1.5 equiv.) was added. The mixture was stirred at room temperature for 8 h and the solvent was removed under the reduced pressure. The residue was partitioned between ethyl acetate and saturated NaHCO₃ solution. The aqueous layer was extracted with ethyl acetate twice, and the combined organic layer was dried over anhydrous Na₂SO₄(s). The filtrate was condensed under reduced pressure and subjected to flash column chromatography. **9aA**: Prepared from **8aA** as a white solid. Yield = 94%; ¹H NMR (400 MHz, CDCl₃) δ 8.36 (s, 2H), 7.26 (d, *J* = 8.6 Hz, 2H), 7.00 (d, *J* = 8.6 Hz, 2H), 6.85 (d, *J* = 8.6 Hz, 2H), 6.78 (d, *J* = 8.6 Hz, 2H), 5.08 (dt, *J* = 6.7, 3.7 Hz, 1H), 4.37–4.27 (m, 3H), 4.14 (s, 2H), 3.85–3.80 (m, 1H), 3.78 (s, 3H), 3.77 (s, 3H), 3.74 (dd, *J* = 8.2, 3.1 Hz, 1H), 3.71–3.68 (m, 1H), 3.23 (s, 6H), 3.04 (s, 3H), 2.35 (brs, 1H); ¹³C NMR (100 MHz, CDCl₃) δ 162.5, 159.7, 159.6, 158.0, 130.4, 130.3, 129.6, 129.0, 118.3, 114.03, 113.99, 82.4, 80.0, 76.5, 75.0, 70.5, 62.7, 55.44, 55.40, 39.0, 37.4; HRMS (FAB+) *m/z* calculated for C₂₇H₃₅N₃O₈S [M+H]⁺: 562.2223; found: 562.2222.

General Synthetic Procedure for *O*-Tritylated Azide-containing Carbohyrids (11). To a stirred solution of **10** (150 mg) and trityl chloride (1.2 equiv.) in anhydrous CH₂Cl₂, diisopropylethylamine (1.5 equiv.) and 4-dimethylaminopyridine (0.1 equiv.) was added. After

1
2
3 stirring at room temperature for 24 h, the mixture was diluted with CH₂Cl₂ and washed with brine.
4
5 The organic layer was dried over anhydrous Na₂SO₄(s) and the filtrate was condensed under
6
7 reduced pressure followed by flash column chromatography. **11aA**: Prepared from **10aA** as a white
8
9 solid. Yield = 88%; ¹H NMR (400 MHz, CDCl₃) δ 8.23 (s, 2H), 7.42–7.40 (m, 6H), 7.29–7.20 (m,
10
11 9H), 7.07 (d, *J* = 8.6 Hz, 2H), 6.86 (d, *J* = 8.6 Hz, 2H), 6.81 (d, *J* = 8.6 Hz, 2H), 6.69 (d, *J* = 8.6
12
13 Hz, 2H), 4.42–4.33 (m, 2H), 4.28 (dd, *J* = 8.0, 2.9 Hz, 2H), 4.06 (d, *J* = 11.0 Hz, 1H), 3.78 (s, 3H),
14
15 3.77 (s, 3H), 3.62 (dd, *J* = 6.7, 5.5 Hz, 1H), 3.50–3.46 (m, 1H), 3.42–3.39 (m, 1H), 3.33–3.28 (m,
16
17 1H), 3.20 (s, 6H); ¹³C NMR (100 MHz, CDCl₃) δ 162.4, 159.34, 159.29, 158.1, 143.8, 130.1,
18
19 129.9, 129.8, 129.5, 128.9, 128.0, 127.2, 117.7, 113.9, 113.7, 87.4, 80.1, 77.8, 74.2, 70.4, 64.1,
20
21 63.2, 55.44, 55.38, 37.4; HRMS (FAB+) *m/z* calculated for C₄₅H₄₆N₆O₅ [M+H]⁺: 751.3608; found:
22
23 751.3604.
24
25
26
27
28

29 **General Synthetic Procedure for *O*-Benzylated Azide-containing Carbohybrids (12).** To a
30
31 stirred solution of **10** (40 mg) in anhydrous dimethylformamide, NaH (2 equiv.) was added slowly
32
33 at 0 °C. After stirring the mixture for 10 min, benzyl bromide (2 equiv.) was added. The reaction
34
35 mixture was stirred for 5 h at room temperature and partitioned between ethyl acetate and water.
36
37 The aqueous layer was extracted with ethyl acetate and the combined organic layer was dried over
38
39 anhydrous Na₂SO₄. The filtrate was condensed under reduced pressure and subjected to flash
40
41 column chromatography. **12aA**: Prepared from **10aA** as a white solid. Yield = 71%; ¹H NMR (400
42
43 MHz, CDCl₃) δ 8.27 (s, 2H), 7.37–7.29 (m, 5H), 7.16 (d, *J* = 8.6 Hz, 2H), 7.02 (d, *J* = 8.6 Hz, 2H),
44
45 6.85 (d, *J* = 8.6 Hz, 2H), 6.77 (d, *J* = 8.6 Hz, 2H), 4.49–4.37 (m, 5H), 4.29 (d, *J* = 5.9 Hz, 1H),
46
47 4.15 (d, *J* = 11.3 Hz, 1H), 3.80 (s, 3H), 3.78 (s, 3H), 3.75–3.74 (m, 1H), 3.66–3.58 (m, 3H), 3.21
48
49 (s, 6H); ¹³C NMR (100 MHz, CDCl₃) δ 162.5, 159.50, 159.45, 158.1, 138.1, 130.2, 129.9, 129.83,
50
51
52
53
54
55
56
57
58
59
60

1
2
3 129.75, 128.6, 127.9, 127.8, 117.9, 114.0, 113.9, 80.5, 77.3, 74.5, 73.5, 70.3, 69.7, 62.1, 55.5, 55.4,
4
5 37.4; HRMS (FAB+) m/z calculated for $C_{33}H_{38}N_6O_5$ $[M+H]^+$: 599.2982; found: 599.2979.
6
7

8 **General Synthetic Procedure for *O*-Mesylated Azide-containing Carbohybrids (13).**
9

10 Triethylamine (3 equiv.) and methanesulfonyl chloride (2 equiv.) were added to a stirred solution
11 of **10** (38 mg) in anhydrous CH_2Cl_2 at 0 °C. The mixture was stirred at room temperature for 3 h,
12
13 diluted with CH_2Cl_2 and washed with brine. The aqueous layer was extracted with CH_2Cl_2 , and
14
15 the combined organic layer was dried over anhydrous $Na_2SO_4(s)$. The filtrate was condensed under
16
17 reduced pressure and subjected to flash column chromatography. **13aA**: Prepared from **10aA** as a
18
19 clear syrup. Yield = 88%; 1H NMR (400 MHz, $CDCl_3$) δ 8.24 (s, 2H), 7.18 (d, J = 8.6 Hz, 2H),
20
21 7.01 (d, J = 8.6 Hz, 2H), 6.87 (d, J = 9.0 Hz, 2H), 6.77 (d, J = 9.0 Hz, 2H), 4.46 (d, J = 11.0 Hz,
22
23 1H), 4.41 (d, J = 11.0 Hz, 1H), 4.35–4.25 (m, 3H), 4.23 (d, J = 7.0 Hz, 1H), 4.16 (d, J = 11.0 Hz,
24
25 1H), 3.88 (dt, J = 8.0, 3.8 Hz 1H), 3.79 (s, 3H), 3.78 (s, 3H), 3.68 (dd, J = 7.0, 4.3 Hz, 1H), 3.23
26
27 (s, 6H), 2.97 (s, 3H); ^{13}C NMR (100 MHz, $CDCl_3$) δ 162.5, 159.7, 159.6, 157.9, 130.2, 130.0,
28
29 129.2, 129.1, 117.6, 114.2, 114.0, 80.5, 76.4, 74.2, 70.3, 69.0, 61.7, 55.44, 55.38, 37.6, 37.4;
30
31 HRMS (FAB+) m/z calculated for $C_{27}H_{34}N_6O_7S$ $[M+H]^+$: 587.2288; found: 587.2289.
32
33
34
35
36
37
38

39 **Biological Materials.** HepG2 (human hepatocellular carcinoma), THP-1 (human monocytic
40
41 leukemia), and U2OS (human osteosarcoma) cells were obtained from American Type Culture
42
43 Collection (ATCC) and cultured in Dulbecco's modified Eagle medium (DMEM) [Gibco]
44
45 containing 10% fetal bovine serum (FBS) [Gibco] and 1% antibiotic-antimycotic solution at 37 °C
46
47 in an atmosphere of 5% CO_2 . BALB/c mice were obtained from The Jackson Laboratory [Bar
48
49 Harbor, ME]. All mice were bred and maintained in specific pathogen-free conditions at the animal
50
51 facility of Institute of Pasteur Korea. All animal experiments were performed with the approval of
52
53 the Institutional Animal Care and Use Committee (IACUC) at IPK (authorization no.
54
55
56
57
58
59
60

1
2
3 IPK05050203IPK-12009). The following materials were purchased from companies in the
4
5 parentheses; hypoxanthine [Sigma-Aldrich], gentamycin [Life Technologies], Albumax [Life
6
7 Technologies], Resazurin [Sigma-Aldrich], Mitotracker Red CMXRos [Life Technologies], and
8
9 wheat germ agglutinin-AlexaFluor488 conjugate [Life Technologies].
10
11

12 **Parasite Lines and Culture Conditions.** *P. falciparum* strain HB3 (Pyr^R), K1 (CQ^R, Pyr^R), and
13
14 W2 (CQ^R, Pyr^R, SDX^R) were obtained from the Biodefense and Emerging Infections (BEI)
15
16 Research Resources [Manassas, VA] and maintained at <10% parasitaemia in human red blood
17
18 cells at 3% hematocrit [blood type O+, Gyeonggi Blood Center, Korean Red Cross]. The culture
19
20 media consisted of RPMI1640, 25 mM HEPES buffer (pH 7.4), 0.1 mM hypoxanthine, 0.016 mM
21
22 thymidine, 0.5% Albumax, and 20 µg/mL gentamycin. Cultures were maintained at 37 °C in
23
24 gassed chambers following injection with a mixture of 5% CO₂, 1% O₂, and 94% N₂. When needed,
25
26 parasites were synchronized at the ring stage by two sorbitol treatments (8-h intervals), and further
27
28 cultivated through one complete cycle prior to the drug activity studies.
29
30
31
32
33

34 **Compound Library and Image-based Parasitological Screening.** An in-house drug-like
35
36 compound library of 3,840 small-molecules that had previously been constructed using a
37
38 privileged substructure-based diversity-oriented synthesis (pDOS) approach was subjected to
39
40 automated high-throughput screening using our novel image-based parasitaemia detection
41
42 method.^{16,17,27} Briefly, DMSO-solubilized test compounds were diluted in complete media and co-
43
44 cultured with *P. falciparum* (K1)-parasitized erythrocytes at a parasitaemia of 1% and hematocrit
45
46 1.5%. The final drug concentrations were 5 µM in a final DMSO amount of 0.5% per well of 50
47
48 µL sample. All liquid-handling procedures were completed using a Biomek's NX robotic station
49
50 (compound dilution), or a CyBi[®] liquid handler (compound transfer), or a Well-Mate dispenser
51
52 (dispensation of parasitized cultures into drugged wells). The cultures were then placed in gassed
53
54
55
56
57
58
59
60

1
2
3 chambers (5% CO₂, 1% O₂, and 94% N₂), and grown for 72 h at 37 °C. Five microliters of each
4
5 well content was transferred into a staining solution comprising wheat germ agglutinin-
6
7 AlexaFluor488 conjugate (RBC membrane stain) and Mitotracker Red CMXRos (mitochondrial
8
9 membrane potential indicator), and maintained at 37 °C for 20 min to allow for complete
10
11 incorporation of the dyes. The resulting cultures were again diluted in fixing solution comprising
12
13 5 µg/mL DAPI and 4%(w/v) paraformaldehyde to a final hematocrit of 0.02% in a 384-well
14
15 imaging plate (black glass-bottom plate, Matrical). Following a 10-min incubation period at room
16
17 temperature, the plates were gently vortexed (1,700 rpm for 30 seconds) and spun at 1,000 rpm for
18
19 1 min to layer the suspended cells onto the well bottom. Five image fields were then acquired from
20
21 each well using an Operetta 2.0 microscopy system that was equipped with a robotic arm and a
22
23 40× objective lens. The acquired images were then submitted for automated image analysis using
24
25 our previously developed image mining algorithms for malaria.¹⁶ Raw data were further exported
26
27 onto an Excel spreadsheet and normalized using the DMSO-only wells as positive growth controls,
28
29 and RBC-only wells as image-mining background.
30
31
32
33
34
35

36 **Hit Selection and Confirmation.** Primary screening hits were defined as reducing the final
37
38 culture parasitaemia by more than 90% when compared to the mean culture parasitaemia in DMSO
39
40 control wells. These primary hits were subjected to dose-response studies against all three drug
41
42 resistant parasite strains to identify those with novel activities. Compounds exhibiting complete
43
44 dose response curves within the analyzed drug range of 0 to 40 µM, and an EC₅₀ less than 2 µM
45
46 were selected for cluster analyses and *in silico* activity searches. Further hit confirmation analysis
47
48 involved compound re-synthesis and antimalarial activity testing in dose-response assays.
49
50
51
52

53 **In Vitro Cytotoxicity Studies.** Compounds were evaluated for cytotoxicity using three human
54
55 cell lines HepG2, THP-1, and U2OS. Cells were seeded at a density of 2,500 cells/well (total
56
57
58
59
60

1
2
3 volume 50 μL) in 384 well plates and incubated for 24 h prior to drug treatment. Two-fold serial
4
5 dilutions of the compounds (starting at 100 μM) were added to the plates and incubated under
6
7 humidified conditions at 37 $^{\circ}\text{C}$ for an additional 48 h. Resazurin (7-hydroxy-3H-phenoxazin-3-
8
9 one-10-oxide) was added to a final concentration of 10 μM and the plates were further incubated
10
11 for 12 h at 37 $^{\circ}\text{C}$. Fluorescence due to the metabolic product of resazurin, resorufin, was measured
12
13 at excitation/emission of 531/572 nm using Victor3 V spectrophotometer [Perkin Elmer]. The
14
15 percent cell viability in each triplicate well was quantified by normalizing against the solvent-
16
17 treated cells using the formula: % Viability = $(uF_{\text{compound}}/uF_{\text{solvent}}) \times 100$, where uF_{compound} is the
18
19 mean resorufin fluorescence in compound-treated wells and uF_{solvent} is the mean fluorescence in
20
21 the solvent-treated wells. Compound concentrations resulting in a 50% (CC_{50}) reduction in cell
22
23 viability was determined by non-linear regression curve fitting using GraphPad Prism 5.04. The
24
25 cytotoxic control wells consisted of serial dilutions of amphotericin B, starting from a final
26
27 concentration of 100 μM and 0.5% final DMSO concentration.
28
29
30
31
32
33

34 **Cytological Profiling of Antimalarial Drug Effects.** The effects of each selected antimalarial
35
36 compound on trophic and schizont development, egress and merozoite invasion, and on the para-
37
38 site mitochondrial membrane potential were determined by high content imaging using a four-time
39
40 point experimental set-up. Synchronized *P. falciparum* (strain HB3)-infected cultures at 1.5%
41
42 hematocrit and 5% parasitaemia were treated for 36 h starting at either the early ring stage (6 hpi),
43
44 late ring stage (18 hpi), or at the late trophozoite (30 hpi) stage with either test or reference
45
46 compounds at a single maximum effect concentrations of 10 μM (i.e. the concentration at which
47
48 no further increase in culture parasitaemia is observed following drug treatment). Drug effects on
49
50 egress and invasion were determined following a 24-h treatment with each compound added at the
51
52 mid-schizont stage (42-hpi). Cultures were sequentially diluted in staining and fixing solutions as
53
54
55
56
57
58
59
60

1
2
3 described above, and imaged using an Operetta 2.0 microscopy system. Following parasite stage
4
5 quantification using our customized image-mining algorithms, stage accumulation index (stage
6
7 proportion in test wells relative to same stage proportion in solvent control wells) were calculated
8
9 and used to assess the rapid acting effects of each compound on trophozoite and schizont
10
11 development *in vitro*. Meanwhile, following the 24-h drug treatment at the 42-hpi, the resulting
12
13 schizont accumulation index was compared against the total parasitaemia reduction index
14
15 (decrease in well parasitaemia relative to control parasitaemia) to distinguish between egress
16
17 inhibition (high schizont accumulation and parasitaemia reduction indices) and drug effects on
18
19 extracellular merozoites (low schizont accumulation index and high parasitaemia reduction index).
20
21 The drug effects on parasite mitochondrial activities were also assessed by comparing the
22
23 proportion of viable (Mitotracker-positive) parasitaemias in drug-treated wells relative to that in
24
25 the solvent controls following a 36-h treatment allowing for early ring development into the
26
27 schizont stage.
28
29
30
31
32

33
34 **Phase I Metabolic Stability Study.** Liver metabolic stability was determined in human and
35
36 mouse liver microsomes. The compound (1 μ M) was mixed with human or rat liver microsomes
37
38 (0.5 mg/mL) [Gentest, BD Biosciences] in 100 mM potassium phosphate buffer (pH 7.4) and
39
40 incubated at 37 °C for 5 min. The reaction was initiated by NADPH regeneration solution [BD
41
42 Biosciences] and terminated by three times volume of ice-cold acetonitrile with imipramine (80
43
44 ng/mL) as internal standard at single-time-point 30 min. After pre-treatment of biological samples
45
46 with vortex and centrifuge, the samples were analyzed by LC/MS/MS system.
47
48
49

50
51 **Pharmacokinetic Study.** The carbohybrid-based antimalarial candidates (**8aA** and **11aA**) were
52
53 administered by intraperitoneal injection (1 and 5 mg/kg) in SD male rats (n = 5). Our candidate
54
55 compounds were prepared as a solution [DMSO, PEG400, Tween 80 and hydroxylpropyl- β -
56
57
58
59
60

1
2
3 cyclodextrin (HP β CD) solution in PBS (final 10% HP β CD) at 10:10:2.5:77.5, v:v:v:v %]. Blood
4
5 samples were taken at 10 and 30 min and at 1, 4, 8, and 24 h post-injection. After the purification
6
7 of plasma by centrifugation, the concentration of carbohybrid-based antimalarial candidates was
8
9 analyzed using Agilent 6460 LC/MS/MS system [Agilent] using electron spray ionization and a
10
11 reverse-phase column [Hypersil GOLD C18, 50 \times 2.1 mm, Thermo Scientific]. Pharmacokinetic
12
13 parameters were obtained after the analysis of plasma concentration-time plot with WinNonlin
14
15 software [Pharsight].
16
17
18

19
20 ***In Vivo* Efficacy Assessment of Antimalarial Drug Candidates 8aA and 11aA.** Compounds
21
22 **8aA** and **11aA** that exhibited potent *in vitro* multi-stage anti-plasmodial activities, selectivity
23
24 indices >600, good metabolic stability and intraperitoneal PK properties were selected for *in vivo*
25
26 efficacy assessment in *Plasmodium chabaudi*-infected BALB/c mice. Each group of five mice was
27
28 infected by i.p. injection of 2×10^7 parasitized erythrocytes per mouse. Twenty-four hours later
29
30 (Day 1), thin smears were prepared from tail blood and used to determine the pre-treatment
31
32 parasitaemias. This was immediately followed by i.p. injection of the compounds to final doses of
33
34 0.03, 0.3, 3, 10, or 30 mg/kg body weights per group. These treatments were repeated for two
35
36 additional days, followed by parasitaemia assessment by light microscopy examination of Giemsa-
37
38 stained thin smears on Day 4 post-infection. Probit analyses of the drug effects were then
39
40 undertaken as previously described.³²⁻³⁴
41
42
43
44
45
46
47
48
49
50
51
52
53
54
55
56
57
58
59
60

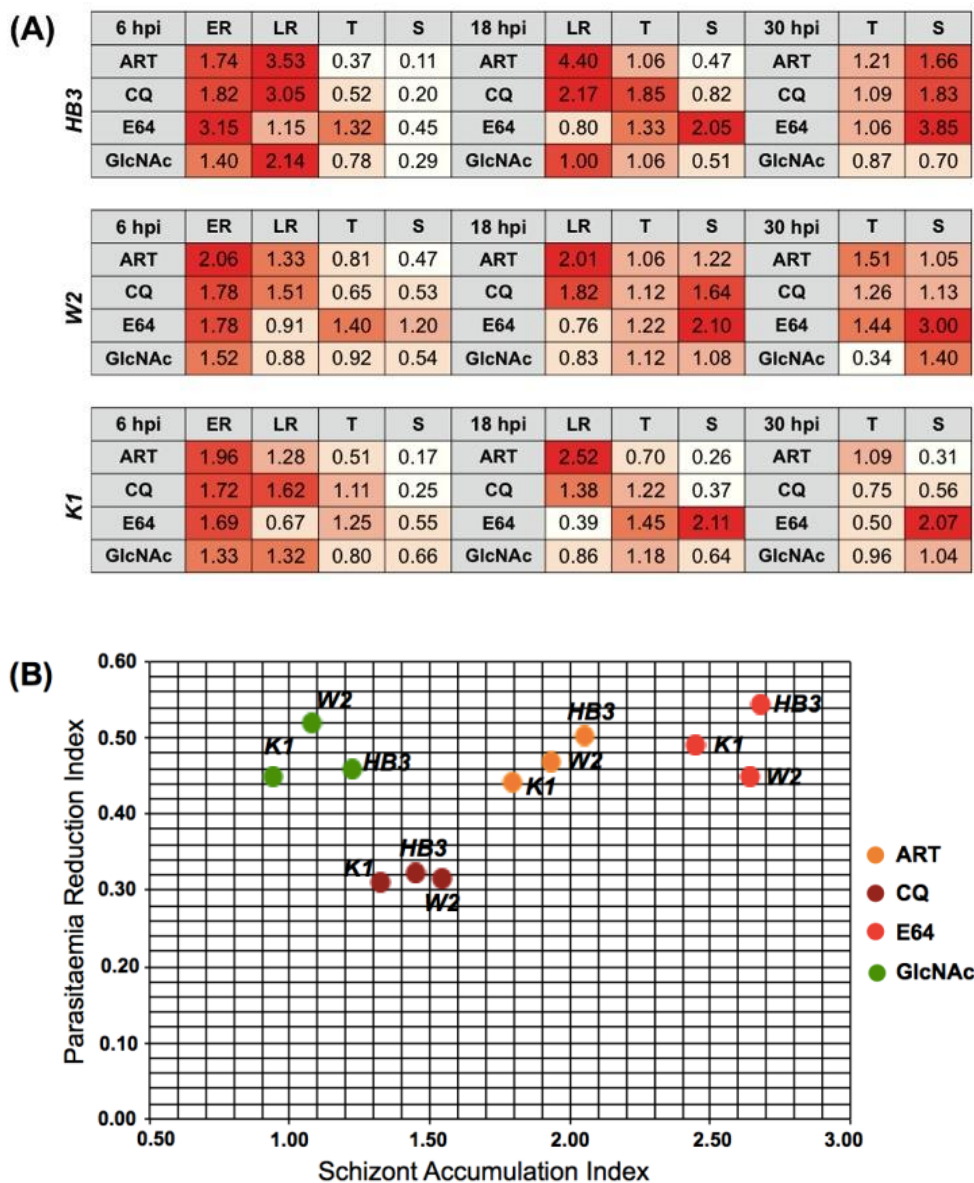


Figure 1. Stage-specific activities of selected antimalarial agents as determined using a novel image-based cytological profiling method. Tightly synchronized *P. falciparum* (HB3, W2 or K1 strains) were treated with 10 μ M final concentration of each antimalarial agent at (A) the 6 hpi (hour post-invasion, early ring), 18 hpi (late ring), or 30 hpi (mid-trophozoite) time-points for a continuous duration of 36 h, or (B) at the 42 hpi time-point (mid-schizont) for 24 h. The parasite nuclei, mitochondria, and host erythrocytes were then stained with DAPI, Mitotracker Red CMXRos, and wheat germ agglutinin AlexaFluor-488, respectively, and the proportion of infected

1
2
3 and viable parasitaemia determined by automated image mining. (A) Heat-map and parasite stage
4 accumulation index at each treatment time-point. ER: Early rings, LR: late rings, T: trophozoites,
5
6 S: schizonts. (B) A plot of parasitaemia reduction index (PRI) against schizont accumulation index
7
8 (SAI) indicating the rapid-acting effects of E64 and artemisinin (ART) on schizonts, and the
9
10 invasion-specific effect (high PRI and low SAI) of *N*-acetylglucosamine (GlcNAc) against all
11
12 three parasite strains. Accumulation or reduction indices greater than the control's mean plus three
13
14 standard deviations ($n = 3$) were considered significant.
15
16
17
18
19
20
21
22
23
24
25
26
27
28
29
30
31
32
33
34
35
36
37
38
39
40
41
42
43
44
45
46
47
48
49
50
51
52
53
54
55
56
57
58
59
60

(A)

6 hpi	ER	LR	T	S	18 hpi	LR	T	S	30 hpi	T	S
ART	2.30	1.20	0.58	0.28	ART	2.87	0.80	0.60	ART	1.60	1.28
E64	1.64	0.61	1.30	1.06	E64	0.87	1.40	2.30	E64	1.42	3.00
GlcNAc	1.40	1.70	0.87	0.40	GlcNAc	0.54	1.12	0.98	GlcNAc	0.86	1.20
1	1.90	2.41	0.88	1.01	1	3.03	1.33	0.67	1	1.71	0.95
2	1.60	1.80	0.60	0.90	2	2.10	1.40	1.10	2	1.70	1.10

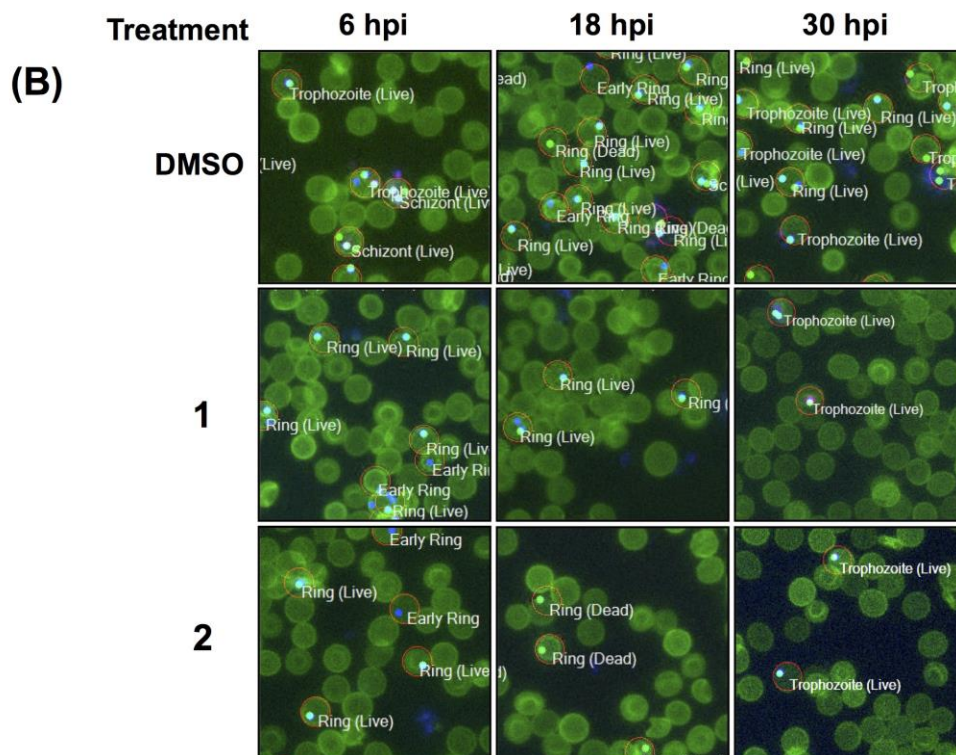


Figure 2. Cellular modes of action of 2-aminopyrimidine-based carbohybrid compounds. Tightly synchronized *P. falciparum* (K1 strain) were treated at the 6 hpi (early ring), 18 hpi (late ring), or 30 hpi (mid-trophozoite) time-points with 10 μ M final concentration **1** or **2** for a continuous duration of 36 h. Parasite nuclei, parasite mitochondrial, and the host erythrocytes were then stained with DAPI, Mitotracker Red CMXRos, and wheat germ agglutinin AlexaFluor-488, respectively, and the proportion of infected and viable parasitaemia determined by automated image analysis. (A) Heat-map and parasite stage accumulation index at each treatment time-point.

1
2
3 ER: Early rings, LR: late rings, T: trophozoites, S: schizonts. (B) Representative images of
4 parasitized cultures showing blockage of further development of "Early Ring", late ring ("Ring"),
5 or "Trophozoite" stage parasites in **1** or **2**-treated cultures compared to the DMSO-treated control.
6
7
8 The mitotracker-positive parasitized erythrocytes are indicated as "Live" whereas mitotracker-
9 negative cells are labeled as "Dead".
10
11
12
13
14
15
16
17
18
19
20
21
22
23
24
25
26
27
28
29
30
31
32
33
34
35
36
37
38
39
40
41
42
43
44
45
46
47
48
49
50
51
52
53
54
55
56
57
58
59
60

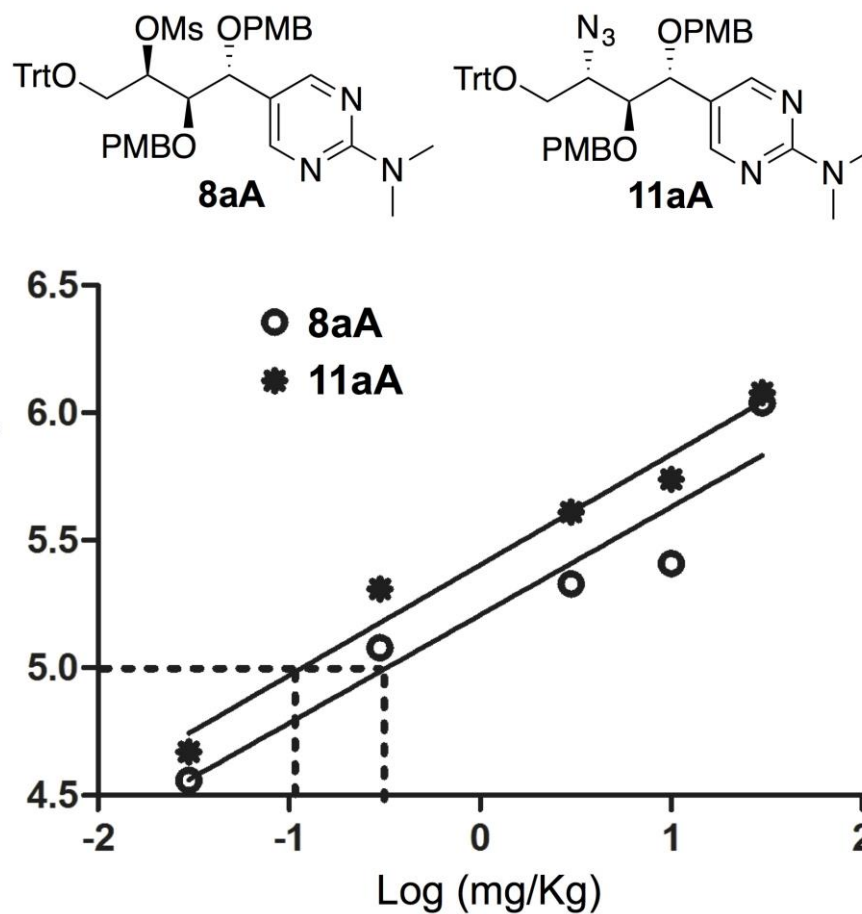
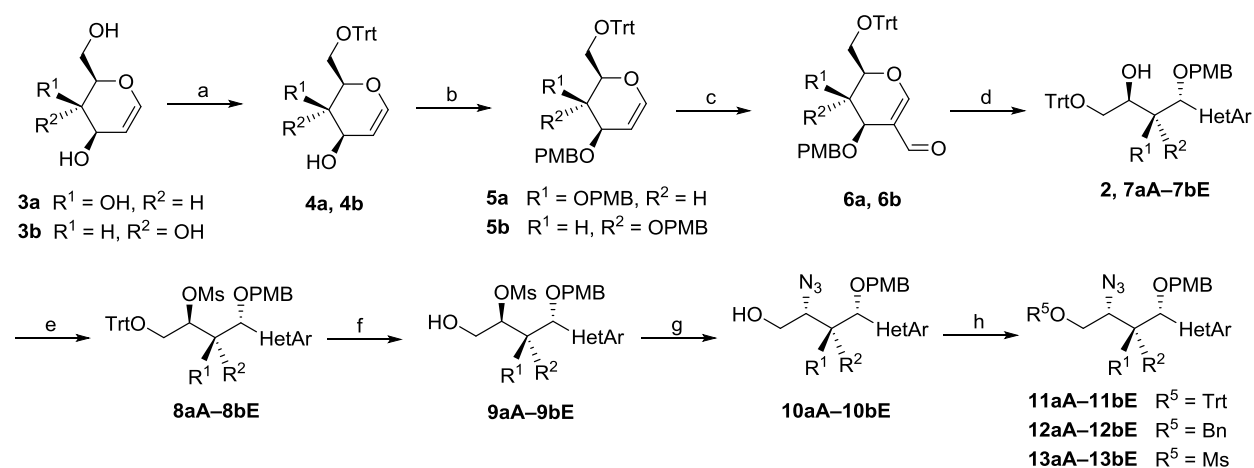


Figure 3. Chemical structures and probit analyses of *in vivo* parasitaemia reduction effects of carbohybrid-based 2-aminopyrimidine **8aA** and **11aA** derivatives. Mice ($n = 5$ per group) were infected with 2×10^7 parasitized erythrocytes per mouse followed by a 3 day treatment from day 1 post-infection with variable doses (0.03, 0.3, 3.0, 10.0, or 30.0 mg/kg body weight) of compound **8aA** or **11aA**. Day 4 parasitaemia were then quantified by light microscopy examination of thin smears, and used in probit plots to analyze the dose-response effects.

Scheme 1. Synthesis of carbohydrate-based molecular frameworks.

Dinucleophile	
HetAr	

Reagents and conditions: (a) TrtCl, DIPEA, DMAP, DCM, rt; (b) PMBCl, NaH, DMF, 0 °C to rt; (c) POCl₃, DMF, 0 °C to rt; (d) Dinucleophiles, K₂CO₃, EtOH/THF, rt; (e) MsCl, TEA, DCM, 0 °C to rt; (f) *p*-TsOH, MeOH, rt; (g) NaN₃, DMF, 120 °C; (h) TrtCl, DIPEA, DCM, rt / BnBr, NaH, DMF, rt / MsCl, TEA, DCM, 0 °C to rt.

Table 1. Antimalarial and cytotoxicity profiles of 2-aminopyrimidine-based hit compounds

Compounds	EC ₅₀ (μM)*			Selectivity Index**
	K1	HB3	W2	
CQ	0.208±0.015	0.033±0.005	0.221±0.012	>450
ART	0.003±0.001	0.018±0.004	0.011±0.001	>5550
1	0.251±0.042	0.442±0.080	0.320±0.038	>226
2	0.535±0.048	0.448±0.061	0.406±0.066	>187

* EC₅₀ values are means±SD of two independent experiments each done in duplicate. **Selectivity indices are calculated as the ratio of 50% cytotoxicity (CC₅₀) values against HepG2 cells to the highest parasitological EC₅₀ values of the three *P. falciparum* strains. The CC₅₀ of amphotericin B (positive cytotoxicity control) was 40±3.2 μM using the resazurin-based assay as described in the “Materials and Methods” section.

Table 2. Antimalarial and cytotoxicity profiles of 2-aminopyrimidine-based hit compounds

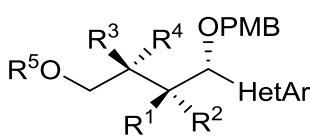
Cpds.							EC ₅₀ (μM) (K1 strain)
	HetAr	R ¹	R ²	R ³	R ⁴	R ⁵	
2	B	OPMB	H	OH	H	Trt	0.351
7aA	A	OPMB	H	OH	H	Trt	0.200
7aC	C	OPMB	H	OH	H	Trt	0.578
7aD	D	OPMB	H	OH	H	Trt	0.352
7aE	E	OPMB	H	OH	H	Trt	0.396
7bA	A	H	OPMB	OH	H	Trt	0.559
7bE	E	H	OPMB	OH	H	Trt	0.478
8aA	A	OPMB	H	OMs	H	Trt	0.116
8aC	C	OPMB	H	OMs	H	Trt	0.225
8aD	D	OPMB	H	OMs	H	Trt	0.160
8aE	E	OPMB	H	OMs	H	Trt	0.158
8bA	A	H	OPMB	OMs	H	Trt	0.198
8bE	A	H	OPMB	OMs	H	Trt	0.237
9aA	A	OPMB	H	OMs	H	H	5.032
10aA	A	OPMB	H	H	N ₃	H	5.447
10aD	D	OPMB	H	H	N ₃	H	18.01
11aA	A	OPMB	H	H	N ₃	Trt	0.092
11aE	E	OPMB	H	H	N ₃	Trt	0.371
11bA	A	H	OPMB	H	N ₃	Trt	0.167
11bE	E	H	OPMB	H	N ₃	Trt	0.281
12aA	A	OPMB	H	H	N ₃	Bn	1.424
12aE	E	OPMB	H	H	N ₃	Bn	1.534
12bA	A	H	OPMB	H	N ₃	Bn	1.197
13aA	A	OPMB	H	H	N ₃	Ms	6.665
13bA	A	H	OPMB	H	N ₃	Ms	11.72
14bA	A	H	OPMB	OH	H	PMB	2.897
15bA	A	H	OPMB	OMs	H	PMB	1.043

Table 3. Microsomal stability and *in vivo* pharmacokinetic properties of candidate compounds **8aA** and **11aA***

Compound	Microsomal stability (% remaining after 30 min, n =3)		PK study (n = 5)				
	Human	Mouse	Dose (mg/kg)	T _{max} (h)	C _{max} (μg/mL)	AUC (μg/mL × h)	T _{1/2} (h)
8aA	88.1±8.01	88.6±5.43	1	1.00±0.00	1.80±0.40	9.79±1.47	10.3±4.62
			5	1.00±0.00	12.9±9.30	41.3±26.1	10.6±12.1
11aA	89.0±7.46	81.6±7.48	1	3.40±1.34	1.03±0.30	8.20±1.62	6.36±0.70
			5	4.00±0.00	3.07±1.03	26.6±8.37	5.78±1.32

*Data represent mean ± SD.

ASSOCIATED CONTENT**Supporting Information**

Supplementary Figures, synthetic procedures, spectroscopic data, ^1H and ^{13}C NMR spectra. This material is available free of charge via the Internet at <http://pubs.acs.org>.

AUTHOR INFORMATION**Corresponding Authors**

Seung Bum Park

E-mail: sbpark@snu.ac.kr. Tel: +8228809090

Lawrence Ayong

E-mail: layong05@yahoo.co.uk. Tel: +23751117600

Author Contributions

†These authors contributed equally.

ACKNOWLEDGMENT

This work was supported by the Creative Research Initiative Grant (2014R1A3A2030423), the Bio & Medical Technology Development Program (2012M3A9C4048780), the Basic Research Laboratory (2010-0019766) funded by the National Research Foundation of Korea (NRF), the National Research Foundation of Korea (NRF) grant funded by the Korea Government (MSIP, No.2007-00559), Gyeonggi-do, and KISTI. D.L. is grateful for a WCU-BK21 Scholarship.

ABBREVIATIONS

ART, artemisinin; CQ, chloroquine; GlcNAc, *N*-acetylglucosamine; hpi, hour post-invasion; ER, Early rings; LR, late rings; T, trophozoites; S, schizonts.

REFERENCES

- (1) Burchard, G. D. [Malaria - update 2013]. *MMW-Fortsch. Medizin* **2013**, *155*, 42–44.
- (2) Lopez Del Prado, G. R.; Hernan Garcia, C.; Moreno Cea, L.; Fernandez Espinilla, V.; Munoz Moreno, M. F.; Delgado Marquez, A.; Polo Polo, M. J.; Andres Garcia, I. Malaria in developing countries. *J. Infec. Dev. Ctries.* **2014**, *8*, 1–4.
- (3) Murray, C. J.; Rosenfeld, L. C.; Lim, S. S.; Andrews, K. G.; Foreman, K. J.; Haring, D.; Fullman, N.; Naghavi, M.; Lozano, R.; Lopez, A. D. Global malaria mortality between 1980 and 2010: a systematic analysis. *Lancet* **2012**, *379*, 413–431.
- (4) Greenwood, B. M.; Fidock, D. A.; Kyle, D. E.; Kappe, S. H.; Alonso, P. L.; Collins, F. H.; Duffy, P. E. Malaria: progress, perils, and prospects for eradication. *J. Clin. Invest.* **2008**, *118*, 1266–1276.
- (5) Chang, H. H.; Moss, E. L.; Park, D. J.; Ndiaye, D.; Mboup, S.; Volkman, S. K.; Sabeti, P. C.; Wirth, D. F.; Neafsey, D. E.; Hartl, D. L. Malaria life cycle intensifies both natural selection and random genetic drift. *Proc. Natl. Acad. Sci. U.S.A.* **2013**, *110*, 20129–20134.
- (6) Wells, T. N.; Alonso, P. L.; Gutteridge, W. E. New medicines to improve control and contribute to the eradication of malaria. *Nat. Rev. Drug Discov.* **2009**, *8*, 879–891.

1
2
3 (7) Dondorp, A. M.; Yeung, S.; White, L.; Nguon, C.; Day, N. P.; Socheat, D.; von Seidlein, L.
4
5 Artemisinin resistance: current status and scenarios for containment. *Nat. Rev. Microbiol.* **2010**, *8*,
6
7 272–280.
8
9

10
11 (8) Verma, R.; Khanna, P.; Chawla, S. Malaria vaccine can prevent millions of deaths in the
12
13 world. *Hum. Vaccin. Immunother.* **2013**, *9*, 1268–1271.
14
15

16
17 (9) Olliaro, P.; Wells, T. N. The global portfolio of new antimalarial medicines under
18
19 development. *Clin. Pharmacol. Ther.* **2009**, *85*, 584–595.
20
21

22
23 (10) Muregi, F. W.; Wamakima, H. N.; Kimani, F. T. Novel drug targets in malaria parasite with
24
25 potential to yield antimalarial drugs with long useful therapeutic lives. *Curr. Pharm. Des.* **2012**,
26
27 *18*, 3505–3521.
28
29

30
31 (11) Enserink, M. If artemisinin drugs fail, what's plan B? *Science* **2010**, *328*, 846.
32
33

34
35 (12) Dondorp, A. M.; Nosten, F.; Yi, P.; Das, D.; Phyoo, A. P.; Tarning, J.; Lwin, K. M.; Ariey,
36
37 F.; Hanpithakpong, W.; Lee, S. J.; Ringwald, P.; Silamut, K.; Imwong, M.; Chotivanich, K.; Lim,
38
39 P.; Herdman, T.; An, S. S.; Yeung, S.; Singhasivanon, P.; Day, N. P.; Lindegardh, N.; Socheat, D.;
40
41 White, N. J. Artemisinin resistance in *Plasmodium falciparum* malaria. *N. Engl. J. Med.* **2009**, *361*,
42
43 455–467.
44
45

46
47 (13) Noedl, H.; Se, Y.; Schaefer, K.; Smith, B. L.; Socheat, D.; Fukuda, M. M. Evidence of
48
49 artemisinin-resistant malaria in western Cambodia. *N. Engl. J. Med.* **2008**, *359*, 2619–2620.
50
51

52
53 (14) Sanz, L. M.; Crespo, B.; De-Cozar, C.; Ding, X. C.; Llergo, J. L.; Burrows, J. N.; Garcia-
54
55 Bustos, J. F.; Gamo, F. J. *P. falciparum* in vitro killing rates allow to discriminate between different
56
57 antimalarial mode-of-action. *PLoS One* **2012**, *7*, e30949.
58
59
60

1
2
3 (15) Grimberg, B. T.; Mehlotra, R. K. Expanding the antimalarial drug arsenal-now, but how?
4
5
6 *Pharmaceuticals (Basel)* **2011**, *4*, 681–712.

7
8
9 (16) Moon, S.; Lee, S.; Kim, H.; Freitas-Junior, L. H.; Kang, M.; Ayong, L.; Hansen, M. A. An
10
11 image analysis algorithm for malaria parasite stage classification and viability quantification. *PLoS*
12
13 *One* **2013**, *8*, e61812.

14
15
16 (17) Oh, S.; Park, S. B. A design strategy for drug-like polyhetero-cycles with privileged
17
18 substructures for discovery of specific small-molecule modulators. *Chem. Commun. (Cambridge,*
19
20 *U.K.)* **2011**, *47*, 12754–12761.

21
22
23 (18) Lim, D.; Park, S. B. Synthesis of molecular frameworks containing two distinct heterocycles
24
25 connected in a single molecule with enhanced three-dimensional shape diversity. *Chem.-Eur. J.*
26
27 **2013**, *19*, 7100–7108.

28
29
30 (19) Zhang, Y.; Asante, K. S.; Jung, A. Stage-dependent inhibition of chloroquine on
31
32 *Plasmodium falciparum* in vitro. *J. Parasitol.* **1986**, *72*, 830–836.

33
34
35 (20) Delves, M. J.; Ruecker, A.; Straschil, U.; Lelievre, J.; Marques, S.; Lopez-Barragan, M. J.;
36
37 Herreros, E.; Sinden, R. E. Male and female *Plasmodium falciparum* mature gametocytes show
38
39 different responses to antimalarial drugs. *Antimicrob. Agents Chemother.* **2013**, *57*, 3268–3274.

40
41
42 (21) Naik, R. S.; Krishnegowda, G.; Gowda, D. C. Glucosamine inhibits inositol acylation of the
43
44 glycosylphosphatidylinositol anchors in intraerythrocytic *Plasmodium falciparum*. *J. Biol. Chem.*
45
46 **2003**, *278*, 2036–2042.

1
2
3 (22) Salmon, B. L.; Oksman, A.; Goldberg, D. E. Malaria parasite exit from the host erythrocyte:
4 a two-step process requiring extraerythrocytic proteolysis. *Proc. Natl. Acad. Sci. U.S.A.* **2001**, *98*,
5 271–276.
6
7
8

9
10
11 (23) Soni, S.; Dhawan, S.; Rosen, K. M.; Chafel, M.; Chishti, A. H.; Hanspal, M.
12 Characterization of events preceding the release of malaria parasite from the host red blood cell.
13 *Blood Cells Mol. Dis.* **2005**, *35*, 201–211.
14
15
16

17
18
19 (24) Klonis, N.; Crespo-Ortiz, M. P.; Bottova, I.; Abu-Bakar, N.; Kenny, S.; Rosenthal, P. J.;
20 Tilley, L. Artemisinin activity against *Plasmodium falciparum* requires hemoglobin uptake and
21 digestion. *Proc. Natl. Acad. Sci. U.S.A.* **2011**, *108*, 11405–11410.
22
23
24

25
26
27 (25) Gligorijevic, B.; Purdy, K.; Elliot, D.; Cooper, R.A.; Roepe P.D. Stage independent
28 chloroquine resistance and chloroquine toxicity revealed via spinning disk confocal microscopy.
29 *Mol. Biochem. Parasitol.* **2008**, *159*, 7–23.
30
31
32

33
34
35 (26) Klonis, N.; Creek, D. J.; Tilley, L. Iron and heme metabolism in *Plasmodium falciparum*
36 and the mechanism of action of artemisinins. *Curr. Opin. Microbiol.* **2013**, *16*, 722–727.
37
38
39

40
41 (27) Singh, K.; Kaur, H.; Smith, P.; de Kock, C.; Chibale, K.; Balza-rini, J. Quinoline-pyrimidine
42 hybrids: synthesis, antiplasmodial activity, SAR, and mode of action studies. *J. Med. Chem.* **2014**,
43 *57*, 435–448.
44
45
46

47
48
49 (28) Zhao, S. High-performance liquid chromatographic determination of artemisinin
50 (qinghaosu) in human plasma and saliva. *Analyst* **1987**, *112*, 661–664.
51
52
53

54
55 (29) White, N.J. Clinical pharmacokinetics and pharmacodynamics of artemisinin and
56 derivatives. *Trans. R. Soc. Trop. Med. Hyg.* **1994**, *88*, 41–43.
57
58
59
60

1
2
3 (30) Krishna, S.; White, N.J. Pharmacokinetics of quinine, chloroquine and amodiaquine.
4
5 Clinical implications. *Clin. Pharmacokinet.* **1996**, *30*, 263-299.
6
7

8
9 (31) SNU3701 and SNU3662 are identical to compound **11b** and **3d**, respectively, in reference
10
11 18.
12

13
14 (32) Berres, M. An effective method for the estimation and comparison of the ED₅₀ with small
15
16 sample sizes. *J. Exp. Anim. Sci.* **1991**, *34*, 21-29.
17
18

19
20 (33) Kelly, G. E.; Lindsey, J. K. Robust estimation of the median lethal dose. *J. Biopharm. Stat.*
21
22 **2002**, *12*, 137-147.
23
24

25
26 (34) Loshadkin, N. A.; Gladkikh, V. D.; Kolosova, N. A.; Sinitsyn, A. N.; Goldenkov, V. A. The
27
28 use of probit-method for an estimation of toxic effects of combined toxicants at low concentration
29
30 levels. *Radiats. Biol. Radioecol.* **2003**, *43*, 337-340.
31
32
33
34
35
36
37
38
39
40
41
42
43
44
45
46
47
48
49
50
51
52
53
54
55
56
57
58
59
60

Table of Contents graphic

